Inorg. Chem. **2007**, *46*, 6723–6732

Chelation of Vanadium(V) by Difluoromethylene Bisphosphonate, a Structural Analogue of Pyrophosphate

Debbie C. Crans,*,† Alvin A. Holder,† Tapan Kumar Saha,† G. K. Surya Prakash,*,‡ Muhammed Yousufuddin,‡ Roman Kultyshev,‡ Rehana Ismail,‡ Myron F. Goodman,*,§ James Borden,£ and Jan Florián*,£,||

Department of Chemistry, Colorado State University, Fort Collins, Colorado 80523, Department of Chemistry, University of Southern California, Los Angeles, California 90089, Department of Biochemistry, University of Southern California, Los Angeles, California 90089, Department of Chemistry, Loyola University, Chicago, Illinois 60626, and Institute of Physics, Charles University, 12116 Prague, Czech Republic

Received December 29, 2006

The structural and functional analogy between difluoromethylene bisphosphonate (CF_2PP) and pyrophosphate (PP_i) is investigated in a reaction with V(V) in the form of vanadate. The reaction of CF_2PP with vanadate was investigated using 1.00 M KCl as supporting electrolyte over the ranges $3 \leq [CF_2PP] \leq 60$ mM and $2.06 \leq pH \leq 11.80$. ^{51}V, ^{19}F, and ^{31}P NMR spectroscopic studies showed that a 1:1 species was formed with an H^+-dependent formation constant of 110 M^{-1} at pH 7.22. Results of solution experiments and ab initio calculations are consistent with CF_2PP coordinating V(V) in a bidentate manner, as previously reported for PP_i. Below pH 4, a minor complex forms, which is consistent with a 1:2 stoichiometry. This complex was also observed with pyrophosphate. The X-ray crystal structure of the monoprotonated difluoromethylene bisphosphonate anion ($H[CF_2PP]^{3-}$)—toludine complex is presented. The $H[CF_2PP]^{3-}$ anion crystallized in the triclinic space group $P\bar{1}$ with $a = 12.7629(7)$ Å, $b = 13.3992(7)$ Å, $c = 17.1002(9)$ Å, and $V = 2584.4(2)$ Å^3, and $Z = 2$. Sheets of the layers of anions are connected through a network of H-bonds and separated by a layer of toludine cations. The structural features are investigated, and the CF_2PP anion was found to be longer and wider than the corresponding PP_i. Given the larger size of this anion compared to PP_i, the chelation affinity upon CF_2 substitution was found to be 4–5-fold reduced at neutral pH.

Introduction

The pyrophosphate unit (abbreviated PP_i) is the key structural and functional component of nucleotide and deoxyribonucleotide diphoshates and triphosphates.[1] Analogues of this unit have been developed for studies of reaction mechanisms and enzyme catalysis.[2−10] Commonly, substitution of the bridged oxygen atom with N, S, or various C-based units are made.[5−10] Such substitutions have a profound effect on the properties of the PP_i system because fundamental parameters such as pK_a values and the metal binding affinity are altered. This work characterizes the fundamental properties of the $[(O_3P)_2CF_2]$ unit, abbreviated CF_2PP, focusing on structural and chelation information for ultimately use in mechanistic studies. The CF_2-substituted

* To whom correspondence should be addressed. E-mail: crans@lamar.colostate.edu (D.C.C.).
† Colorado State University.
‡ Department of Chemistry, University of Southern California.
§ Department of Biochemistry, University of Southern California.
£ Loyola University.
|| Charles University.

(1) Nelson, D. L.; Cox, M. M. *Lehninger Principles of Biochemistry*. 3rd ed.; Worth Publishers: New York, 2000.
(2) Batra, V. K.; Beard, W. A.; Shock, D. D.; Krahn, J. M.; Pedersen, L. C.; Wilson, S. H. *Structure* **2006**, *14*, 757−766.
(3) Barabas, O.; Pongracz, V.; Kovari, J.; Wilmanns, M.; Vertessy, B. G. *J. Biol. Chem.* **2004**, *279*, 42907−42915.
(4) Stefan, C.; Jansen, S.; Bollen, M. *Purinergic Signalling* **2006**, *2*, 361−370.
(5) Blackburn, G. M.; Eckstein, F.; Kent, D. E.; Perree, T. D. *Nucleoside, Nucleotide Nuclic Acids* **1985**, *4*, 165−7.
(6) Ma, Q. F.; Kenyon, G. L.; Markham, G. D. *Biochemistry* **1990**, *29*, 1412−16.
(7) Rizk, S. S.; Cuneo, M. J.; Hellinga, H. W. *Protein Sci.* **2006**, *15*, 1745−1751.
(8) Soti, C.; Vermes, A.; Haystead Timothy, A. J.; Csermely, P. *Eur. J. Biochem.* **2003**, *270*, 2421−2428.
(9) Boyle, N. A.; Fagan, P.; Brooks, J. L.; Prhavc, M.; Lambert, J.; Cook, P. D. *Nucleoside, Nucleotide Nuclic Acids* **2005**, *24*, 1651−1664.
(10) Li, R.; Muscate, A.; Kenyon, G. L. *Bioorg. Chem.* **1996**, *24*, 251−261.

10.1021/ic062484r CCC: $37.00
Published on Web 07/12/2007

PP_i, CF_2PP, has pK_a values of 1.44, 2.11, 5.66, and 7.63,[11] which compare well to that of PP_i of 0.85, 1.49, 5.77, and 8.22.[12] We have chosen to study the complexation of CF_2-PP with vanadium(V) (V(V) in the form of vanadate) because ^{51}V NMR spectroscopy is a sensitive probe[13] and the corresponding studies with vanadate have been detailed for PP_i.[12] The comparison of trianionic difluoromethylene bisphosphonate, $H[(O_3P)_2CF_2]^{3-}$, abbreviated $H[CF_2PP]^{3-}$, with PP_i on the ability to form complexes with vanadate may provide important information on the interactions of these derivatives with metal ions and the potential difference in how CF_2 analogues act in enzymes catalyzing phosphoryl transfer.

PP_i commonly acts as a bidentate ligand for metal ions.[14−27] Protonation of PP_i leads to mono-, di-, and triprotonated PP_i that have very different chelation properties. Although stable complexes form with phosphate, complexes formed from PP_i are much more stable, reflecting the fact that most of these complexes contain the PP_i ligands coordinated in a bidentate manner.[27,28] Strong complexes form between PP_i and metal ions such as magnesium, calcium, iron, cobalt, and other transition metal ions.[14,15,18,19,21,23,25−34] When PP_i chelates a metal ion in a bidentate manner, the phosphate groups are eclipsed and the internal P−O bond and the bite angles determine the fit between anion and the metal ion. The reaction between vanadate and PP_i forms two complexes, the most stable being a 1:1 (V/PP_i) complex.[12] A 1:2 species with a central octahedral V atom chelated to two PP_i moieties was proposed as a minor species.[12] An interesting V complex has been reported containing both V(III) and V(IV).[35] The V(IV) in the form of a vanadyl cation (VO^{2+}) is coordinated in a bidentate manner to PP_i, and the V(III) serve as counter cations associated with neutralization of the overall charge of the complex.[35] The cyclic nature of the $VO^{2+}-PP_i$ complex is analogous to that reported for $Mg^{2+}-PP_i$.[27,36]

The reaction of CF_2PP, with vanadate generates one major 1:1 product analogous to the major product formed with PP_i. The presence of the electron-withdrawing CF_2 group increases the first two pK_a values and should decrease this analogues affinity for metal ions. However, given the complexity of the system a quantitative comparison based on pK_a values is not straightforward. We provide experimental data demonstrating that PP_i's affinity for a metal ion at neutral pH decreases by a factor 4−5 when the bridging oxygen atom is substituted with CF_2.

Experimental Section

Materials. All reagents were of analytical grade (Sigma Aldrich). Ultrapure water, obtained by deionizing distilled water using a Nanopure water system, was used for preparative work and to make up solutions for all physical measurements.

Synthesis of Difluoromethylene Bisphosphonic Acid. (a) Synthesis of Tetraethyl Difluoromethylenediphosphonate. The synthesis of tetraethyl difluoromethylenediphosphonate was based on a modified procedure by Shipitshin et al.[37] Scheme 1S. In a typical preparation, a 100 mL Schlenk flask equipped with a magnetic stirbar and rubber septum was charged under dry nitrogen with THF (10 mL, freshly distilled from sodium benzophenone ketyl) and *i*-Pr_2NH (1.80 mL, 12.8 mmol, freshly distilled from NaOH) and placed in ice−water bath. After 30 min of stirring, a 2.45 M *n*-BuLi solution in hexanes (5.30 mL, 13.7 mmol) was added dropwise within 6 min. After another 30 min, the ice−water bath was replaced by a −78 °C isopropanol−dry ice slush bath, and the reaction mixture was stirred for an additional 30 min before a solution of diethyl difluoromethyl phosphonate[38] (2.26 g, 12.0 mmol) in THF (9 mL) was added dropwise within 6 min. Thirty minutes later, a solution of diethyl phosphochloridate (2.05 g, 11.9 mmol) in THF (9 mL) was added dropwise to the brown reaction mixture within 8 min. After 1 h of stirring at −78 °C, the isopropanol−dry ice bath was replaced by an ice−water bath and stirring was continued for another hour before a saturated aqueous solution of KH_2PO_4 (10 mL) was added to the reaction mixture. After being stirred at ambient temperature overnight, the contents of the flask were transferred into a separatory

(11) Burton, D. J.; Pietrzyk, D. J.; Ishihara, T.; Fonong, T.; Flynn, R. M. *J. Fluorine Chem.* **1982**, *20*, 617−626.
(12) Gresser, M. J.; Tracey, A. S.; Parkinson, K. M. *J. Am. Chem. Soc.* **1986**, *108*, 6229−6234.
(13) Crans, D. C.; Smee, J. J.; Gaidamauskas, E.; Yang, L. *Chem. Rev.* **2004**, *104*, 849−902.
(14) Angenault, J.; Couturier, J. C.; Quarton, M.; Robert, F. *Eur. J. Solid State Inorg. Chem.* **1995**, *32*, 335−343.
(15) Balic-Zunic, T.; Christoffersen, M. R.; Christoffersen, J. *Acta Crystallogr., Sect. B: Struct. Sci.* **2000**, *B56*, 953−958.
(16) Beaury, L.; Derouet, J.; Binet, L.; Sanz, F.; Ruiz-Valero, C. *J. Solid State Chem.* **2004**, *177*, 1437−1443.
(17) Bettach, M.; Benkhouja, K.; Zahir, M.; Rissouli, K.; Sadel, A.; Giorgi, M.; Pierrot, M. *Acta Crystallogr., Sect. C: Cryst. Struct. Commun.* **1998**, *C54*, 1059−1062.
(18) Boudin, S.; Grandin, A.; Labbe, P.; Grebille, D.; Nguyen, N.; Ducouret, A.; Raveau, B. *J. Solid State Chem.* **1996**, *121*, 291−300.
(19) Boutfessi, A.; Boukhari, A.; Holt, E. M. *Acta. Crystallogr., Sect. C: Cryst. Struct. Commun.* **1996**, *C52*, 1594−1597.
(20) Byrappa, K.; Dutt, B. V. U.; Clearfield, A.; Poojary, M. D. *J. Mater. Res.* **1994**, *9*, 1519−1525.
(21) Calvo, C.; Au, P. K. L. *Can. J. Chem.* **1969**, *47*, 3409−3416.
(22) Alaoui, E. B.; Boukhari, A.; Holt, E. M. *Acta. Crystallogr., Sect. C: Cryst. Struct. Commun.* **1994**, *C50*, 482−484.
(23) El, Khayati, N.; Rodriguez-Carvajal, J.; Bouree, F.; Roisnel, T.; Cherkaoui, R.; Boutfessi, A.; Boukhari, A. *Solid State Sci.* **2002**, *4*, 1273−1283.
(24) Gali, S.; Byrappa, K.; Gopalakrishna, G. S. *Acta Crystallogr., Sect. C: Cryst. Struct. Commun.* **1989**, *C45*, 1667−1669.
(25) Lii, K. H.; Shih, P. F.; Chen, T. M. *Inorg. Chem.* **1993**, *32*, 4373−4377.
(26) Maass, K.; Glaum, R. *Acta Crystallogr., Sect. C: Cryst. Struct. Commun.* **2000**, *C56*, 404−406.
(27) Souhassou, M.; Lecomte, C.; Blessing, R. H. *Acta Crystallogr., Sect. B: Struct. Sci.* **1992**, *B48*, 370−376.
(28) Haromy, T. P.; Linck, C. F.; Cleland, W. W.; Sundaralingam, M. *Acta Crystallogr., Sect. C: Cryst. Struct. Commun.* **1990**, *C46*, 951−957.
(29) Boutfessi, A.; Boukhari, A.; Holt, E. M. *Acta Crystallogr., Sect. C: Cryst. Struct. Commun.* **1996**, *C52*, 1597−1599.
(30) Haromy, T. P.; Knight, W. B.; Dunaway-Mariano, D.; Sundaralingam, M. *Biochemistry* **1982**, *21*, 6950−6956.
(31) Sperow, J. W.; Butler, L. G. *J. Biol. Chem.* **1976**, *251*, 2611−2612.
(32) Leclaire, A.; Borel, M. M.; Grandin, A.; Raveau, B. *J. Solid State Chem.* **1988**, *76*, 131−135.
(33) Mahesh, M. J.; Gopalakrishna, G. S.; Ashamanjari, K. G.; Prasad, J. S. *Indian J. Phys.* **2005**, *79*, 37−40.
(34) Chudinova, N. N.; Murashova, E. V.; Ilyukhin, A. B.; Tarnopol'skii, V. A.; Yaroslavtsev, A. B. *Inorg. Mater.* **2005**, *41*, 69−72.
(35) Johnson, J. W.; Johnston, D. C.; King, H. E.; Halbert, T. R.; Brody, J. F. *Inorg. Chem.* **1988**, *27*, 1646−1648.
(36) Oka, J.; Kawahara, A. *Acta Crystallogr., Sect. B: Struct. Sci.* **1982**, *B38*, 3−5.
(37) Shipitshin, A. V.; Victorova, L. S.; Shirokova, E. A.; Dyatkina, N. B.; Goryunova, L. E.; Beabealashvilli, R. S.; Hamilton, C. J.; Robetrs, S. M.; Krayevsky, A. *J. Chem. Soc., Perkin Trans. 1* **1999**, 1039−1050.
(38) Bergstrom, D. E.; Shum, P. W. *J. Org. Chem.* **1988**, *53*, 3953−3958.

Table 1. Crystal Data and Structure Refinement for $C_{44}H_{60}F_4N_6O_{12}P_4$

empirical formula	$C_{44}H_{60}F_4N_6O_{12}P_4$
fw	1064.86
cryst color, habit	
crystal dimens (mm^3)	0.25 × 0.20 × 0.10
temp (K)	153(2)
wavelength (Å)	0.71073
cryst syst	triclinic
space group	$P\bar{1}$
formula unit/unit cell	1
a (Å)	12.7629(7)
b (Å)	13.3992(7)
c (Å)	17.1002(9)
α (°)	69.350(2)
β (°)	72.000(2)
γ (°)	89.762(3)
V ($Å^3$)	2584.4(2)
Z	2
density (calcd) (Mg/m^3)	1.370
abs coeff (mm^{-1})	0.224
F(000)	1118
2θ range (°)	$1.35 \le 2\theta \le 27.10$
range of h, k, l	$-16 \rightarrow 13, -16 \rightarrow 17, -22 \rightarrow 13$
reflns collected	15 683
independent reflns	10 969 [R(int) = 0.0373]
completeness to $\theta = 27.10°$	96.2%
abs correction	none
refinement method	full-matrix least-squares on F^2
data/restraints/params	10 969/0/647
GOF on F^2	1.006
final R indices [$I > 2\sigma(I)$]	R1 = 0.0484, wR2 = 0.0879
R indices (all data)	R1 = 0.0805, wR2 = 0.0932
largest diff. peak and hole	0.480 and −0.346 e.$Å^{-3}$

funnel with aid of EtOAc (80 mL) and water (40 mL). The aqueous phase was washed twice with 50 mL portions of EtOAc, and the organic phases were combined and dried over $MgSO_4$. After filtration and removal of solvent and any volatiles under reduced pressure the crude product was obtained as yellow oil. It was purified by column chromatography on silica gel (EtOAc/hexanes, 3:2). Additional purification was achieved by heating the product under vacuum (75 °C, 3 mmHg) for 17 h. The product was a colorless oil, yield 2.71 g (70%). ^{1}H NMR (400 MHz, $CDCl_3$): δ 4.28−4.40 (8H, m, OCH_2), 1.38 (12 H, t, $J = 7.0$, CH_3). ^{19}F NMR (376 MHz, $CDCl_3$, external reference $CFCl_3$ in $CDCl_3$): δ −122.0 (t, J_{P-F} = 86.1). ^{31}P{^{1}H} NMR (162 MHz, $CDCl_3$, external reference = 85% H_3PO_4): δ 4.2 (t, $J_{P-F} = 86.0$).

(b) Synthesis of Difluoromethylene Bisphosphonic Acid. The synthesis of difluoromethylene bisphosphonic acid (H_4CF_2PP) was done according to a modified procedure of McKenna and Shen,[39] Scheme 1S. In a typical synthesis, a 50 mL round-bottomed flask containing tetraethyl difluoromethylenediphosphonate (2.68 g, 8.27 mmol) and a magnetic stirbar was charged under dry nitrogen with 98% bromotrimethylsilane (7.00 mL, 52.0 mmol). The flask was sealed with a glass stopcock, and the reaction mixture was stirred at ambient temperature for 4.5 days. The volatiles were removed in vacuo followed by addition of water (14 mL). After being stirred for 50 min at ambient temperature, the colorless liquid was transferred into a separatory funnel, and the organic phase was separated and discarded. The aqueous phase was washed twice with 15 mL portions of ether and transferred into a 100 mL round-bottomed flask with water (combined volume 30 mL). Most of water was removed in vacuo at ambient temperature. The resulting oil was dried over P_2O_5 in vacuo (0.1 mmH*g*, 4 days), the wet P_2O_5 being replaced with fresh dry material at least once. H_4CF_2-PP: colorless crystals, yield 1.68 g (96*%*). ^{19}F NMR (376 MHz, D_2O, external reference $CFCl_3$ in $CDCl_3$): δ −123.0 (t, J_{P-F} = 85.2). ^{31}P{^{1}H} NMR (162 MHz, D_2O, external reference = 85% H_3PO_4): δ 4.1 (t, $J_{P-F} = 85.4$). The sodium salt of difluoromethylene bisphosphonic acid was prepared using the method reported by Burton et al.[11]

(39) McKenna, C.; Shen, P. *J. Org. Chem.* **1981**, *46*, 4573−4576.

Table 2. Selected Bond Lengths (Å) and Angles (deg) for $C_{44}H_{60}F_4N_6O_{12}P_4$

P(1)−O(1)	1.5052(15)	P(2)−O(6)	1.4995(17)
P(1)−O(3)	1.5156(17)	P(2)−O(5)	1.5641(19)
P(1)−O(2)	1.5209(15)	P(2)−C(1)	1.849(2)
P(1)−C(1)	1.866(3)	F(1)−C(1)	1.382(2)
P(2)−O(4)	1.4965(17)	F(2)−C(1)	1.396(2)
O(1)−P(1)−O(3)	113.87(10)	O(4)−P(2)−C(1)	104.78(10)
O(1)−P(1)−O(2)	113.47(09)	O(6)−P(2)−C(1)	108.34(10)
O(3)−P(1)−O(2)	111.83(09)	O(5)−P(2)−C(1)	103.60(10)
O(1)−P(1)−C(1)	107.18(10)	F(1)−C(1)−F(2)	104.61(17)
O(3)−P(1)−C(1)	106.05(10)	F(1)−C(1)−P(2)	107.13(15)
O(2)−P(1)−C(1)	103.49(10)	F(2)−C(1)−P(2)	108.67(15)
O(4)−P(2)−O(6)	116.59(11)	F(1)−C(1)−P(1)	108.26(15)
O(4)−P(2)−O(5)	109.80(11)	F(2)−C(1)−P(1)	107.88(15)
O(6)−P(2)−O(5)	112.60(10)	P(2)−C(1)−P(1)	119.34(12)

Synthesis of Sodium Difluoromethylene Bisphosphonate (Na_4CF_2PP). Solid H_4CF_2PP (0.307 g, 1.45 mmol) and Na_2CO_3 (0.307 g, 2.89 mmol) were mixed in a 100 mL beaker; then deionized water (10 mL) was added to the mixture. Dissolution caused effervescence, with evolution of CO_2. The mixture was gently heated on a hotplate to remove water at ∼80 °C resulting in a white solid. The beaker and its contents were placed in an oven set at 110 °C so as to make the anhydrous salt, sodium CF_2PP. Yield = 0.413 g (95%). Analysis: ESI MS (negative mode): m/z = 211.00 {$[HO(O)_2PCF_2P(O)(OH)_2]^-$}. ^{31}P NMR {10% D_2O, pH 7.06, and I = 1.00 M (KCl)}: δ 6.26 (t).

Preparation of the *m*-Toludinium Salt of Difluromethylene Bisphosphonic Acid for Crystallographic Analysis. Difluoromethylene bisphosphonic acid (Tol_4CF_2PP) (50 mg, 0.33 mmol) was dissolved in deionized water (10 mL). The solution was treated with excess *m*-toludine (0.500 mL, 4.67 mmol) under stirring. A sticky brown precipitation formed. The precipitate was recrystallized from deionized water, and crystals were grown in deionized water for X-ray analysis.

X-ray Crystallography. Diffraction data for the $H[CF_2PP]^{3-}$ anion were collected at 153 K on a SMART APEX CCD diffractometer with graphite-monochromated Mo K_α radiation (λ = 0.71073 Å). A hemisphere of the crystal data was collected up to a resolution of 0.75 Å. Cell parameters were determined using SMART software. The SAINT package was used for integration of data, Lorentz, polarization, and decay corrections, and for the merging of data. No absorption correction was applied. All calculations for structure determination were carried out using the SHELXTL package (version 5.1). Initial atomic positions were located by direct methods using XS, and the structure was refined by least-squares methods using SHELX with 10 969 independent reflections and within the range of $\theta = 1.35-27.10°$ (completeness 96.2%). Calculated hydrogen positions were input and refined in a riding manner along with the attached carbons. Hydrogen atoms involved in H-bonding were located using the appropriate HFIX command. Views of the structure were prepared using ORTEP3 for Windows. Additional details of the data collection and refinement for the crystal of the $H[CF_2PP]^{3-}$ anion studied are given in Table 1. Fractional coordinates are given in Table 2, and selected bond lengths and angles are given in Table 3.

Preparation of Solutions for Spectroscopic Studies. The vanadate stock solutions (∼103 mM) were prepared by dissolving $NaVO_3$ in deionized water in volumetric flasks. The exact concentration of the stock solution was determined at pH 13 by UV/visible

Table 3. Selected Bond Lengths and Angles for $H[(O_3P)_2CF_2]^{3-}$ ($H[CF_2PP]^{3-}$) and Related PP_i and Calculated Species[27,35]

complex	$H[(O_3P)_2CF_2]^{3-}$ ($H[CF_2PP]^{3-}$)	$H[(O_3P)_2O]^{3-}$	$[(O_3P)_2O]^{4-}$	$[(O_3P)_2O]^{4-}$	$H[(O_3P)_2CF_2]^{3-}$ ($H[CF_2PP]^{3-}$) calcd	$H[(O_3P)_2O]^{3-}$ calcd	$CF_2P_2O_8V^{3-}$ (cyclic) calcd
cation	*m*-toludinium	guanidinium	VO^{2+}, V^{3+}	Mg^{2+}	Na^+	Na^+	Na^+
P−O (brid)	−	1.621(8) 1.626(6)	1.597(3)	1.620(4)	−	1.68	−
P−C (brid)	1.866(3)/ 1.849(2)	−	−	−	1.88/1.87	−	1.87/1.88
P═O/P−O(ter)	1.4965(17)/ 1.5209(15)	1.478(8)/ 1.514(7)	1.484(5)	1.493(4)/ 1.520(4)	1.54	1.54	1.52
P−OH	1.5641(19)	1.550(7) 1.536(8)	−	−	1.64	1.63	−
P−O (cation)	1.4995(17)	1.514(7)	1.562(6)	1.507(4)/ 1.520(4)	1.52	1.52	1.61
<O−P−O (bridging)	−	102.8(3)−109.7(4) (135.9° av)	104.2(4)	102.8(2)−107.1(2)	−	102.0	−
<O−P−C (bridging)	103.49(10)	−	−	−	102.0/100.6	−	101.2
<P−O−P (bridging)	−	128.2(4)	127.8(7)	125.6(2)	−	127.6	−
<P−C−P (bridging)	119.34(12) (119.8° av)	−	−	−	122.9	−	120.0
refs	this work	47	36	28	this work	this work	this work

spectroscopy at 260 nm with a molar extinction coefficient of 3.55×10^3 M^{-1} cm^{-1}.[40]

Solutions for the ^{51}V NMR spectra were prepared at the desired pH values, ligand, and vanadate concentrations using stock solutions containing each component. First, a sufficient amount of the stock solution of the ligand was added for the desired pH; then a sufficient stock solution of sodium vanadate was added to give the desired V(V) concentration, and finally, sufficient KCl was added to give a final ionic strength of 1.0 M. If needed, the pH was adjusted to the desired value with either 0.01 M NaOH or 0.01 M HCl.

NMR Spectroscopy. ^{51}V NMR spectra were acquired on a INOVA-400 MHZ at 105.2 MHz with the spectral window of 299.6 kHz, a pulse angle of 60°, and an acquisition time of 0.080 s with no relaxation delay. A 15 Hz exponential line broadening was applied before Fourier transformation except in the case of line width measurements. Mole fractions of vanadate species were measured using Origin 7 SR4, V 7.0 software and applying the Lorentz function. $VOCl_3$ was used as an external reference for all ^{51}V NMR spectra.[41] Assuming that all the V present in solution was in the form of V(V), the relative intensities of the V(V) species were used to calculate the concentrations of each specific V-containing species (V_1 monomer; V_2 dimer; V_4 tetramer; V_5 pentamer; complexes).

^{31}P NMR spectra were acquired on a Varian INOVA-300 spectrometer at 121.5 MHz the spectral window of 10.0 kHz, a pulse angle of 60°, and an acquisition time of 1.60 s with no relaxation delay. A sample containing 85% H_3PO_4 in D_2O was used as an external reference for all ^{31}P NMR spectra.

^{19}F NMR spectra were acquired on a Varian INOVA-300 spectrometer at 282.4 MHz with the spectral window of 50.0 kHz, a pulse angle of 60°, and an acquisition time of 0.300 s with no relaxation delay. A sample containing 500 mM KF in D_2O was used as an external reference for all ^{19}F NMR spectra.

Quantum Mechanical Calculations. A B3LYP gradient-corrected hybrid density functional[42,43] was used in conjunction with the integral equation formalism implementation of the polarized continuum model (IEF-PCM)[44] with the 6-31G* split-valence polarized basis set. The triple-ζ valence polarized (TZVP) basis set of Ahlrichs[45] was used for V(V) to more accurately describe its d orbitals. This method will be further denoted as IEF-PCM/B3LYP/6-31G*. All geometry optimizations were done at the IEF-PCM/B3LYP/6-31G* level under loose criterion (opt = loose) using the Gaussian 03 program.[46] IEF-PCM was used to generate an environment reproducing dielectric properties of water. Na^+ counterions were placed about calculated structures in order to produce a total charge of zero for the studied systems to improve the reliability of the applied computational methods. These calculations were carried out for monoprotonated pyrophosphate, $H[(O_3P)_2O]^{3-}$, and the CF_2 analogue, $H[(O_3P)_2CF_2]^{3-}$, ions, as well as for the products of the reaction of monoprotonated $H[(O_3P)_2CF_2]^{3-}$ with vanadate, leading to several cyclic and linear conformers of the resulting 1:1 complexes. The topology, numbering scheme, and Cartesian coordinates for the singly and doubly protonated pyrophosphate and CF_2 analogues, as well as the vanadate and CF_2 analogue products, are given in the Supporting Information (Figures 1S and 2S, Table 1S).

Relative free energies of the cyclic and linear conformers of 1:1 CF_2PP−V(V) complexes in aqueous solution were determined as a difference in the IEF-PCM/B3LYP/6-31G* energies, which

(40) Newman, L.; La Fleur, W. J.; Brousaicles, F. J.; Ross, A. M. *J. Am. Chem. Soc.* **1958**, *80*, 4491−4495.
(41) Jaswal, J. S.; Tracey, A. S. *Inorg. Chem.* **1991**, *30*, 3718−3722.
(42) Lee, C.; Yang, W.; Parr, R. G. *Phys. Rev. B* **1988**, *37*, 785−789.
(43) Becke, A. D. *J. Chem. Phys.* **1993**, *98*, 5648−5652.
(44) Mennucci, B.; Cances, E.; Tomasi, J. *J. Phys. Chem. B* **1997**, *101*, 10506−10517.
(45) Schafer, A.; Horn, H.; Ahlrichs, R. *J. Chem. Phys.* **1992**, *97*, 2571−2577.
(46) Frisch, M. J.; Trucks, G. W.; Schlegel, H. B.; Scuseria, G. E.; Robb, M. A.; Cheeseman, J. R.; Montgomery, J. A., Jr.; Vreven, T.; Kudin, K. N.; Burant, J. C.; Millam, J. M.; Iyengar, S. S.; Tomasi, J.; Barone, V.; Mennucci, B.; Cossi, M.; Scalmani, G.; Rega, N.; Petersson, G. A.; Nakatsuji, H.; Hada, M.; Ehara, M.; Toyota, K.; Fukuda, R.; Hasegawa, J.; Ishida, M.; Nakajima, T.; Honda, Y.; Kitao, O.; Nakai, H.; Klene, M.; Li, X.; Knox, J. E.; Hratchian, H. P.; Cross, J. B.; Bakken, V.; Adamo, C.; Jaramillo, J.; Gomperts, R.; Stratmann, R. E.; Yazyev, O.; Austin, A. J.; Cammi, R.; Pomelli, C.; Ochterski, J. W.; Ayala, P. Y.; Morokuma, K.; Voth, G. A.; Salvador, P.; Dannenberg, J. J.; Zakrzewski, V. G.; Dapprich, S.; Daniels, A. D.; Strain, M. C.; Farkas, O.; Malick, D. K.; Rabuck, A. D.; Raghavachari, K.; Foresman, J. B.; Ortiz, J. V.; Cui, Q.; Baboul, A. G.; Clifford, S.; Cioslowski, J.; Stefanov, B. B.; Liu, G.; Liashenko, A.; Piskorz, P.; Komaromi, I.; Martin, R. L.; Fox, D. J.; Keith, T.; Al-Laham, M. A.; Peng, C. Y.; Nanayakkara, A.; Challacombe, M.; Gill, P. M. W.; Johnson, B.; Chen, W.; Wong, M. W.; Gonzalez, C.; Pople, J. A. *Gaussian 03*, revision C.02; Gaussian, Inc.: Wallingford, CT, 2004.

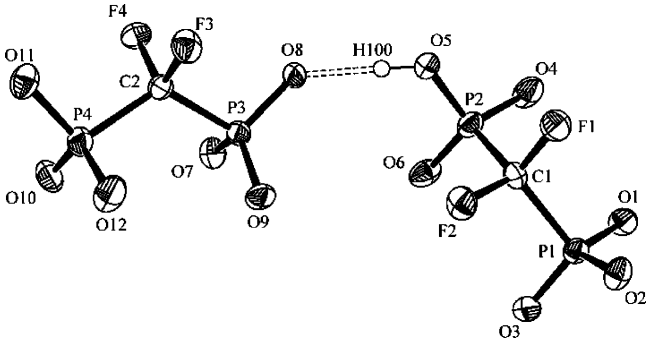

Figure 1. Two molecules of $H[(O_3P)_2CF_2]^{3-}$ interconnected through a H-bond. This dimeric unit forms a superstructure of sheets connected through a H-bonding pattern.

included gas phase, electrostatic solute−solvent interactions, and nonelectrostatic (cavitation) terms. For each molecule, the lowest energy from the three independent calculations that differed in the initial positions of Na^+ counterions was used. Solute−solvent boundaries for the IEF-PCM calculations were generated using Pauling's atomic radii (1.2, 1.35, 1.4, 1.57,1.5, 1.7, and 1.8 Å for H, F, O, Na, C, V, and P atoms, respectively).

Results and Discussion

Synthesis of Difluoromethylene Bisphosphonate Anion. Preparation of various salts of the title anion has previously been reported.[11,39] In our hands these procedures produce several products, so we provide a modified approach to the preparation of the title anion with less side products and higher yield.

X-ray Crystal Structure of the Monohydrogen CF_2PP Anion. The crystallographic data and selected structural parameters for the $H[CF_2PP]^{3-}$ anion are given in Tables 1 and 2. The structural information on the counterion, toludine, showed no unusual structural parameters. The structure for the anion is shown in Figures 1 and 3S. Since the bond lengths for the bridging P−C bonds are longer (av = 1.858 Å) than the P−O bonds (av = 1.597 Å), the $[CF_2PP]^{4-}$ anion is significantly longer than the corresponding PP_i anion.[47] The shape of the anion is slightly different since the bite angle <P−O−P is different from that of the <P−C−P. The F atoms in the CF_2 unit are occupying the position of the lone pairs in the PP_i unit and contribute to increasing the size of the $[CF_2PP]^{4-}$ unit compared to the PP_i.

Since the objective of this work is to compare the PP_i unit with the CF_2PP unit, structural parameters are given in Table 3 for selected PP_i anions. Although the anion can coordinate in a monodentate fashion,[47] the bidentate coordination mode is far more common.[27,35] An initial comparison between anions show that the P═O and P−O(Cation) bonds are similar between the two series of systems. The P−OH is longest for the PP_i unit, but the major differences observed are in the bridging unit and the <P−O−P/<P−C−P angles.[47] The calculated P−O bond lengths of PP_i are 1.68 Å, whereas the calculated P−C bonds of CF_2PP are 1.87 Å. The calculated bridging angle <P−O−P of PP_i is 127.6° whereas the calculated bridging angle <P−C−P of CF_2PP is 122.9°. The CF_2PP unit is therefore longer and bulkier than PP_i.

Under biological conditions, PP_i is generally coordinated in a bidentate manner to metal ions such as magnesium.[27] The main difference between the monoprotonated PP_i anion and the $H[CF_2PP]^{3-}$ is size. Therefore, a detailed comparison of the trianionic PP_i and CF_2PP with the PP_i bound to magnesium or vanadium[27,35] document the subtle differences such as the bond length of the P−OH bond (1.5725(18)/1.536(8) Å) or the P−O(cation) (1.562(6) Å compared to about 1.52 Å for most P−O bonds. Interestingly, the bite angles of the magnesium complex are very similar to the V complex. These structures show that the longer Mg−O bond length is being balanced by the longer P−O(cation) in the V complex, suggesting that such change is more favorable rather than changes in the bite angle.

Since two $[(O_3P)_2CF_2]^{4-}$ molecules crystallized very close together, the possibility for some kind of interaction was investigated. A probable hydrogen-bonding scheme was observed between a protonated phosphate and a terminal phosphate group in a different molecule (see Figure 1). Calculating hydrogen atoms in the usual riding manner is circumspect for hydroxyl groups. However, using an appropriate HFIX command, we were able to locate some electron density around an oxygen atom and assign hydrogen to it. Figure 1 shows the H-bonding between H100 from one anion and O8 from another. The O8−H100 distance was found to be 1.64(3) Å, which is well within the distances commonly observed in hydrogen bonds. The dimeric units combine to make a super structure with sheets of anions linked by H-bonding between units.

Charge Distribution of the Protonated PP_i and CF_2PP Anions. Atomic charges were calculated to reproduce IEF-PCM/B3LYP/6-31G* electrostatic potentials of mono- and diprotonated PP_i and CF_2PP anions in complexes with Na^+ ions in aqueous solution. These charges are presented in Table 1S of the Supporting Information. Since the total charge of the $-CF_2-$ group (−0.26 a.u.) is less negative than the charge of the bridging −O− group in PP_i (−0.48 a.u.), there is an excess negative charge of −0.22 a.u. that is distributed on the remaining part of the CF_2PP anion. The calculations indicate that the excess negative charge is moved mainly to phosphorus atoms, which are significantly less positive in CF_2PP than in PP_i. This redistribution is consistent with the P−C bond having more covalent character than the corresponding P−O bond.

Reaction of Vanadate with Difluoromethylene Bisphosphonate: ^{51}V NMR Studies. The reaction of vanadate (V_1) with CF_2PP was first examined as a function of pH at 5 mM V_i, 60 mM CF_2PP_t, and I = 1.0 M (KCl), Figure 2. At pH 11.80 and 9.89, two species are observed, the major species being HVO_4^{2-} (δ −536, line width 44 Hz) and the minor species being $V_2O_7^{4-}$ (δ −560). No evidence for redox processes were observed in any of the studies reported in this manuscript. These species are labeled in Figure 2 as V_1 and V_2, respectively. With further decrease in pH to 8.90, signals for V_1 (δ −541) and V_2 (δ −565 and −571)

(47) Adams, J. M.; Ramdas, V. *Acta Crystallogr., Sect. B: Struct. Sci.* **1976**, *32*, 3224−3227.

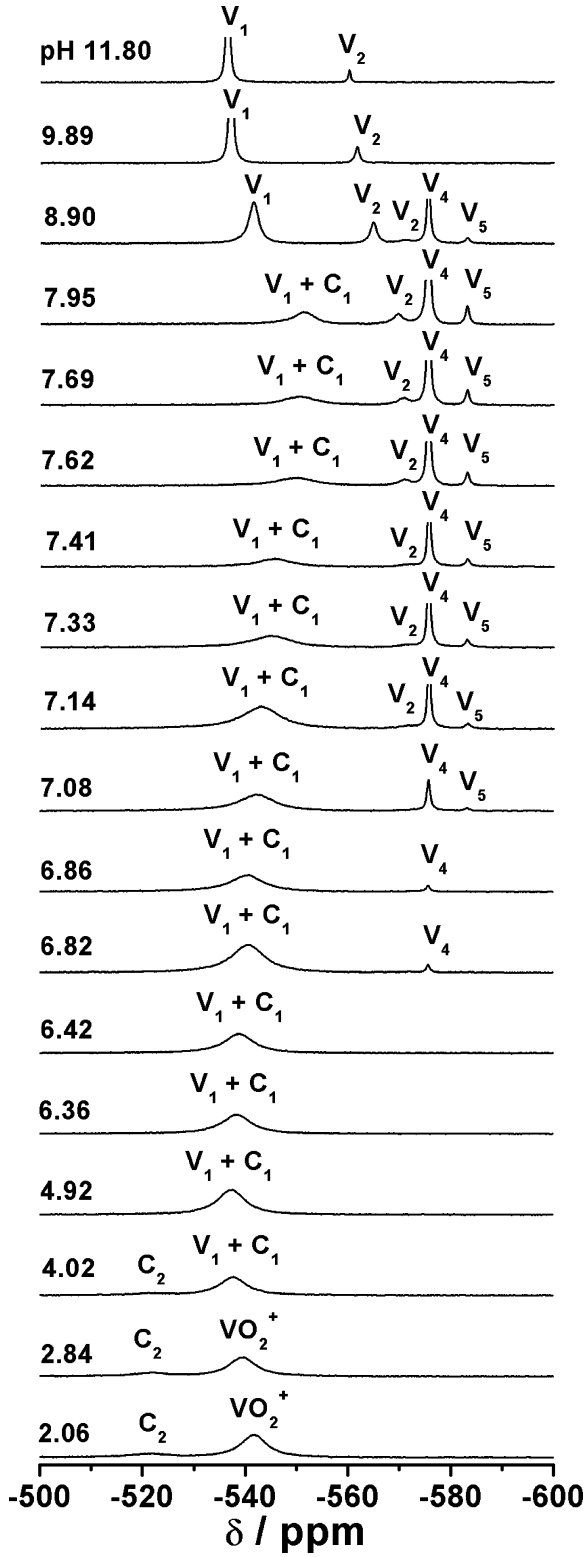

Figure 2. ^{51}V NMR spectra recorded of CF_2PP and vanadate solutions as pH is varied from 2.06 to 11.80. The vanadate oligomers monomer (V_1), dimer (V_2), tetramer (V_4), and pentamer (V_5) are labeled. Complexes (C_1 and C_2) are also indicated. $[V_t] = 5.00$ mM, $[CF_2PP_i] = 60.0$ mM, and $I = 1.00$ M (KCl).

shift and other oligomeric vanadates are observed including V_4 (tetramer at δ −576), and V_5 (pentamer at δ −583). The V_1 signal is broadened to 233 Hz as a result of protonation to form $H_2VO_4^-$. At pH 7.95, further broadening of this signal is accompanied by further shifting of the signal

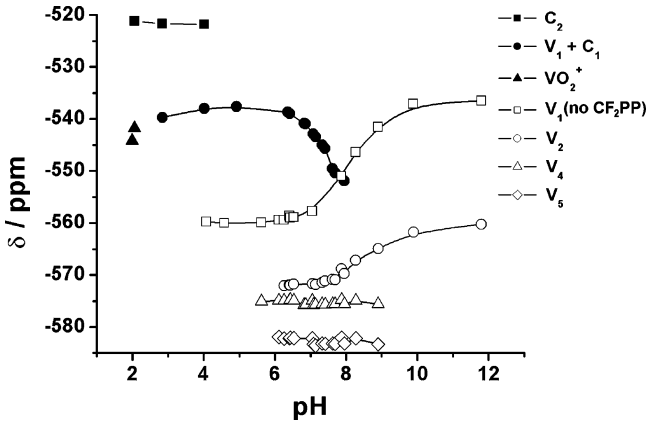

Figure 3. ^{51}V NMR chemical shifts are shown as a function of pH of vanadate and CF_2PP solutions at 1.00 M KCl. The chemical shifts are indicated for the vanadate oligomers (V_1, V_2, V_4, V_5) and V_1 (as either $H_2VO_4^-$ or HVO_4^{2-}) in the absence of CF_2PP.

downfield (δ −552, line width 485 Hz). The broadening of this signal is much more than can be attributed by protonation of the V_1 species and is consistent with complex formation between vanadate and the CF_2PP ligand overlapping the V_1 signal. The signal superposition of vanadate and complex was as previously observed with the complex formed with PP_i.[12] With continued decrease of pH, this signal continues to increase accompanied by broadening and shift of this signal from δ −552 to −539 (line width 726 Hz) at pH 6.42, where this signal is the only vanadate species present.

Since a complex between vanadate and CF_2PP forms at lower pH, characterization of the system was also carried out in the acidic pH range as shown in Figure 2. As the pH decreases from 6.36 to 4, two signals (δ −523 and −538) were observed in the presence of CF_2PP. These two peaks persisted even at pH values as low as 2.06, but the minor signal at δ −522 does not form in the absence of CF_2PP. The signal at δ −542 (line width 662 Hz) has shifted slightly at pH 2.06. However, at even lower pH this signal is solely attributed to the VO_2^+ ion (at δ −544, line width 532 Hz) as can readily be confirmed in solutions containing only V(V).

The plot of the ^{51}V NMR chemical shift of the reaction mixture as a function of pH visually illustrates complex formation, see Figure 3. In this figure the chemical shift of vanadate under similar conditions is given for comparison and the existence of complex is apparent when the observed chemical shift deviate from that of vanadate alone.

Analysis and Stoichiometry of the Complexes Formed between Vanadate and CF_2PP. The reaction of vanadate with CF_2PP was investigated further at pH 7.22 to determine the formation constant and stoichiometry for the complex that forms with vanadate. In Figure 4, selected ^{51}V NMR spectra are shown of a study in which the concentration of CF_2PP is varied at pH 7.22 at a total vanadate concentration of 5.00 mM and at $I = 1.00$ M (KCl). The V_1 signal at δ −557 (line width 122 Hz) is shifted downfield and dramatically broadened as CF_2PP is added. At 5 mM the CF_2PP the signal is observed at δ −554 and the line width is 1140 Hz. The signal continues to shift as the concentration

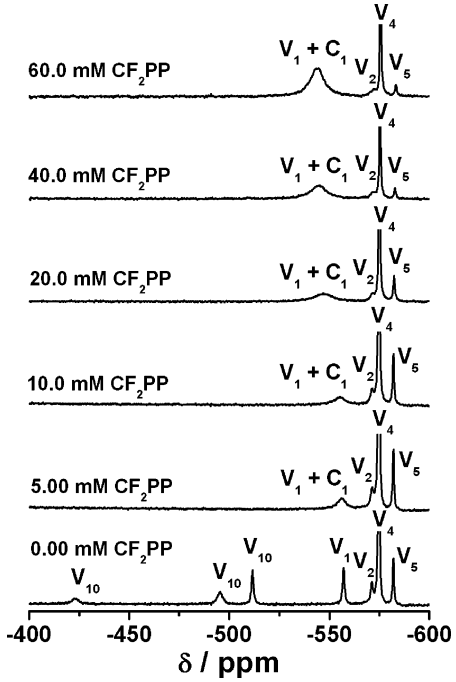

Figure 4. ^{51}V NMR spectra of CF_2PP and vanadate solutions as concentration of CF_2PP is varied. The complex (C_1), V_1, V_2, V_4, V_5, and decavanadate (V_{10}) species are indicated on the spectra. [V_t] = 5.00 mM, pH = 7.22, and I = 1.00 M (KCl).

of CF_2PP increase (at δ −543 at 60 mM CF_2PP), and at the same time, the line width of the signal decrease from 1140 to 826 Hz. At the higher concentrations of CF_2PP, a signal attributed to the V_2 oligomer also begins to broaden, presumably reflecting the chemical exchange taking place with the V_1 species. We conclude that the observations for the CF_2PP system are qualitatively similar to those reported for the PP_i system.[12]

The nature of the complex that forms from vanadate reacting with CF_2PP shown in Figures 3 and 4 were analyzed using the approach reported previously for PP_i. The equilibria are given in eqs 1−5.[12,48,49] A 1:1 complex and a 1:2 complex, as shown in eqs 4−5, are considered.

$$V_4 \overset{K_0}{\rightleftharpoons} 2V_2 \quad (1)$$

$$V_2 \overset{K_1}{\rightleftharpoons} 2V_1 \quad (2)$$

$$V_5 \overset{K_2}{\rightleftharpoons} 5V_1 \quad (3)$$

$$V_1 + CF_2PP \overset{K_3}{\rightleftharpoons} V(CF_2PP) \quad (4)$$

$$V(CF_2PP) + CF_2PP \overset{K_4}{\rightleftharpoons} (CF_2PP)V(CF_2PP) \quad (5)$$

The total V(V) concentration, V_t, can be expressed as shown in eq 6, and the concentration of a 1:1 and a 1:2 complex is given as shown in eqs 7 and 8. Assuming that

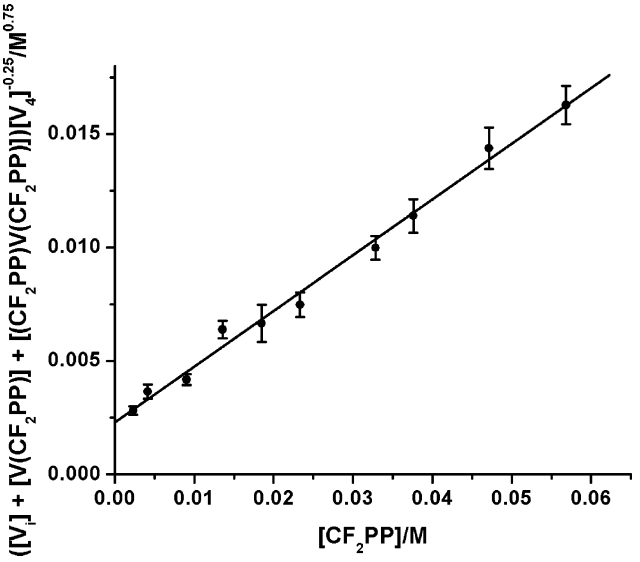

Figure 5. Plot of the sum of V_1 and V−CF_2PP complex near δ −543 as a function of [CF_2PP]. [V_t] = 5.00 mM, [CF_2PP_t] = 0−60.0 mM, pH = 7.22, and I = 1.00 M (KCl).

the δ −543 signal in the study carried out at pH 7.22 (Figure 4) consists of signals from V_1, a 1:1 complex ($V(CF_2PP)$) and a 1:2 complex ($(CF_2PP)V(CF_2PP)$), by virtue of identical in chemical shift, or rapid chemical exchange, eq 9 can be written from a combination of eqs 6−8.

$$V_t = [V_5] + [V_4] + [V_2] + [V_1] + [V(CF_2PP)] + [(CF_2PP)V(CF_2PP)] \quad (6)$$

$$[V(CF_2PP)] = K_3[CF_2PP][V_1] = K_3K_1^{1/2}K_0^{1/4}[CF_2PP][V_4]^{1/4} = K_3K_1^{1/2}[CF_2PP][V_2]^{1/2} \quad (7)$$

$$[(CF_2PP)V(CF_2PP)] = K_4K_3K_1^{1/2}K_0^{1/4}[CF_2PP]^2[V_4]^{1/4} = K_4K_3K_1^{1/2}[CF_2PP]^2[V_2]^{1/2} \quad (8)$$

$$([V_1] + [V(CF_2PP)] + [(CF_2PP)V(CF_2PP)])/[V_4]^{1/4} = K_1^{1/2}K_0^{1/4} + K_3K_1^{1/2}K_0^{1/4}[CF_2PP] + K_4K_3K_1^{1/2}K_0^{1/4}[CF_2PP]^2 \quad (9)$$

A plot of the left-hand side of eq 9 versus [CF_2PP] will give an intercept of $K_1^{1/2}K_0^{1/4}$. If no $(CF_2PP)V(CF_2PP)$ is present in solution, the line will be straight with a slope of $K_3K_1^{1/2}K_0^{1/4}$; otherwise it will have an upward curvature. A plot of the left-hand side of eq 9 versus [CF_2PP] is shown in Figure 5, and since an intercept is observed, we deduce that no $(CF_2PP)V(CF_2PP)$ complex forms at pH 7.22. The slope was calculated as 0.25 $M^{-1/4} = K_3K_1^{1/2}K_0^{1/4}$, while the intercept was 2.3×10^{-3} $M^{3/4}$, which is equal to $K_1^{1/2}K_0^{1/4}$. The ratio of slope to intercept, K_3, can be calculated to be 110 M^{-1} on the basis of the four V atoms in the V_4 species. K_0 and K_1 are calculated as 8.6×10^{-4} and 1.8×10^{-4} M, respectively, at pH 7.22 and I = 1.0 M (KCl).

$$([V_1] + [V(CF_2PP)] + [(CF_2PP)V(CF_2PP)])/[V_2]^{1/2} = K_1^{1/2} + K_3K_1^{1/2}[CF_2PP] + K_4K_3K_1^{1/2}[CF_2PP]^2 \quad (10)$$

(48) Crans, D. C.; Willging, E. M.; Butler, S. R. *J. Am. Chem. Soc.* **1990**, *112*, 427−432.
(49) Crans, D. C.; Schelble, S. M.; Theisen, L. A. *J. Org. Chem.* **1991**, *56*, 1266−1274.

Equations similar to eq 9 can be written in terms of $[V_2]$ instead of $[V_4]$ so that an independent measure of K_1 and K_3 is deduced. Equation 10 is analogous to eq 9. A plot of the left-hand side of eq 10 versus $[CF_2PP]$ is given in the Supporting Information (Figure 4S), where the intercept is equal to 1.4×10^{-2} $M^{1/2}$, which is equal to $K_1^{1/2}$. The slope is $K_3K_1^{1/2} = 3.1$ $M^{-1/2}$. From the ratio of slope to intercept, K_3 was calculated as 230 M^{-1}, which corresponds to a value of 120 M^{-1} for K_3 (based on two V atoms in the dimeric species). The values for K_3 as calculated from eqs 9 and 10 are 110 and 120 M^{-1}, showing consistency within the data.

We obtained a K_3 at an average of 110 M^{-1} at pH 7.22 and $I = 1.0$ M (KCl) which compares to a $K_3 = 39.0$ M^{-1} for PP_i reported by Gresser et al.[12] at pH 7.98, 20 mM Tris-chloride, and $I = 1.0$ M (KCl). Thus, although the concentration of the CF_2PP used to observe the complex were higher than needed for PP_i, comparison of the data shows that the formation constant of CF_2PP is higher than that observed for PP_i. This seeming contradiction is due to the fact that these complexes are pH dependent and more stable at lower pH. Thus, a direct comparison between the two systems required that measurements were done for PP_i at pH 7.22; the possibility of conducting the analysis with CF_2PP at pH 8 was less desirable because the stability of this complex rapidly decreased above pH 7. Using the similar approach, the experiments were repeated for PP_i at pH 7.22 and a pH-dependent formation constant of 500 M^{-1} for K_3 was obtained. These results are consistent with CF_2PP being a 4−5-fold poorer metal ion chelator than PP_i.

Often the ligands' pK_a values are used to obtain such a quantitative comparison of complex stability. In general, such qualitative analysis works when the reacting ligand pK_a and the product pK_a change in concert. In the case of CF_2PP and PP_i, such analysis is more difficult to carry out because the ligands have several pK_a values, and presumably the species in solution and the species that is forming complex both contribute to the formation constant. Since the pairs of pK_a values being for CF_2PP[11] and PP_i 1.44/0.85, 2.11/1.49, 5.66/5.77, and 7.63/8.22, the comparison for this system is nontrivial and would not lead to a quantitative comparison as described above using the chelation constants.

The complex at −522 ppm appears only below pH 4. A concentration study was carried out at pH 1.9 to explore this complex further (see Supporting Information, Figure 5S). At this pH the concentration of the 1:1 complex described above is negligible (Figure 2 and 3). Analysis of the data at pH 1.9 using eq 8 and plotting concentration of complex as a function of $[CF_2PP]^2[V_1]$ produces a straight line at low concentration followed by saturation of complex at higher $[CF_2PP]$ (see Supporting Information, Figure 5S). This behavior is consistent with this minor complex being of a 1:2 stoichiometry with one V(V) and two CF_2PP ligands resulting in a formation constant of 3×10^3 M^{-2}. Analogous species were reported for the PP_i in the pH range 1−2.5 using UV/vis spectroscopy.[50] The form of CF_2PP chelated to the V(V) was previously suggested to be protonated.[50]

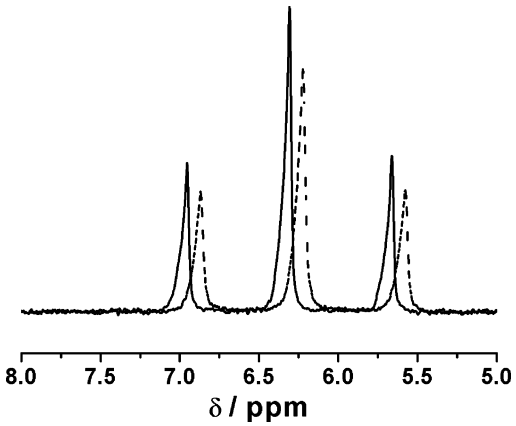

Figure 6. ^{31}P NMR spectra of 60 mM CF_2PP in the absence (—) and presence (− − −) of 5 mM vanadate at pH 7.07 and $I = 1.0$ M (KCl).

Reaction between Vanadate with Difluoromethylene Bisphosphonate: ^{31}P and ^{19}F NMR Studies. The reaction of vanadate with CF_2PP was also followed as a function of pH using ^{31}P and ^{19}F NMR spectroscopy. The ^{31}P NMR spectra of CF_2PP show a triplet over the entire pH range in the presence and absence of vanadate. The J(PF) coupling constant is 78 Hz for both spectra, shown in Figure 6. The main difference between the two sets of spectra in the presence and absence of vanadate is the chemical shift for the signals. At pH 7 a significant amount of complex is present in solution in rapid exchange with free ligand. This is evident from the different chemical shift observed for the solution containing ligand and vanadate compared to the solution containing only ligand (Figure 6). Because the system is in fast exchange with a 10-fold excess of ligand to V(V), only a small fraction of the chemical shift difference (between free ligand and complex) is observed. This difference of 0.1 ppm at a 10-fold excess of ligand corresponds to a chemical shift difference of about 2 ppm between ligand and complex, which cannot be observed, as the temperature cannot be lowered enough without freezing. Differences of 5 ppm are observed when phosphate is derivatized by alkylation, or protonation, whereas metal ion chelation of PP_i derivatives results in a shift of about 2 ppm.[51,52] A smaller chemical shift difference is also consistent with the complex having a condensed triphosphate-like character and reports found with other metal ions chelating PP_i or triphosphate.[51,52]

The reaction of vanadate with CF_2PP as a function of pH was studied by ^{19}F NMR spectroscopy from pH 11.65 to 2.06 (Figure 7a). Since these species vary as a function of pH, the J(FP) coupling constant was measured to be 78 Hz both in the presence (Figure 7a) and absence (Figure 7b) of vanadate. The sharp triplet at pH 11.65 broadened and the chemical shifts changed with the protonation of the CF_2PP as the pH was decreased. In addition to the changes as a result of the protonation reactions, additional changes take place once vanadate is introduced. Since no further peaks are observable, such changes are consistent with a free ligand

(50) Leitsin, V. A.; Grekov, S. D.; Sirina, T. P.; Pritsker, B. S. *Zh. Neorg. Khim.* **1972**, *17*, 1325−1330.

(51) Bose, R. N.; Viola, R. E.; Cornelius, R. D. *J. Am. Chem. Soc.* **1984**, *106*, 3336−3343.

(52) Knorre, D. G.; Lebedev, A. V.; Levina, A. S.; Rezvukhin, A. I.; Zarytova, V. F. *Tetrahedron* **1974**, *30*, 3073−3079.

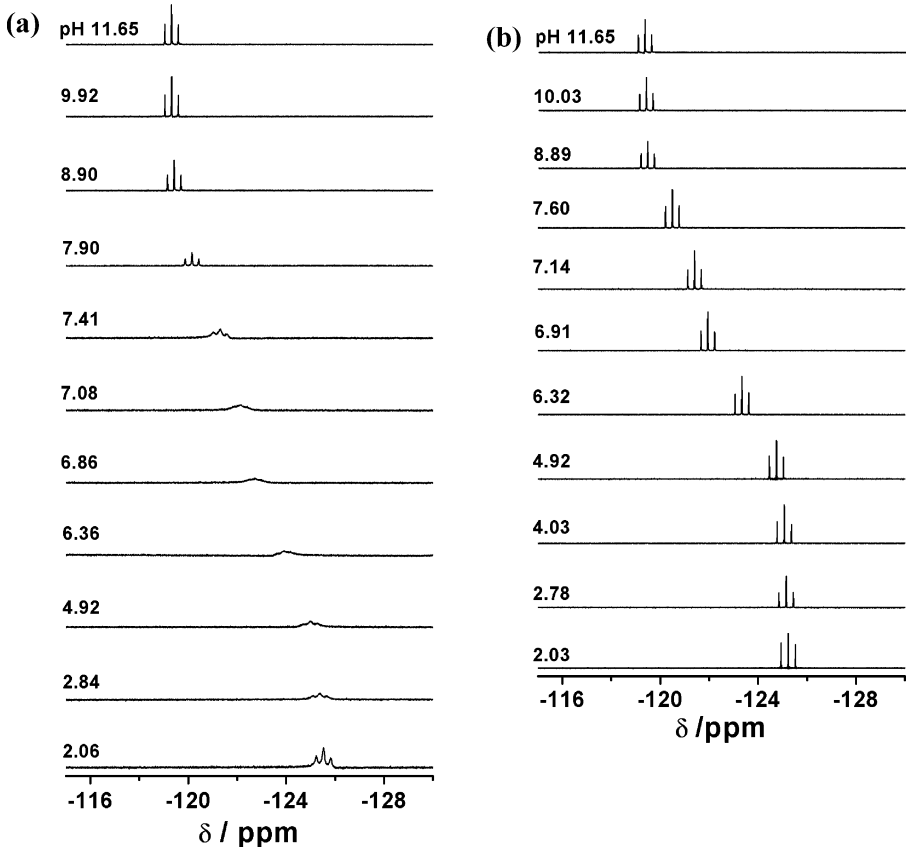

Figure 7. ^{19}F NMR spectra of 60 mM CF_2PP in the presence (A) and absence (B) of 5 mM vanadate as pH is varied at $I = 1.0$ M (KCl).

and complex in rapid exchange.[53] The broadening of the spectra in the presence of vanadate shows the presence of an additional dynamic process: the formation and breakup of the complex.

These interpretations were confirmed by ^{19}F and ^{51}V variable-temperature NMR experiments, the data obtained at pH 7.4 are shown in the Supporting Information (Figures 6S and 7S). As the temperature decreased, the chemical shifts changed slightly for free ligand, but corresponding changes were not observed for the sample containing vanadate (Figure 6S). This observation is consistent with formation of a complex in rapid equilibrium. When subjecting these samples to ^{51}V NMR studies (Figure 7S), the studies at 0 °C show a distinctive signal broadening consistent with a system in which the signals were approaching coalescence at −3 °C, the lowest temperature we were able to run.

From a plot of the ^{19}F NMR chemical shifts versus pH, pK_{a3} and pK_{a4} can be calculated as 5.4 and 7.1, respectively, at an ionic strength of 1.0 M (KCl). These values are close to those reported previously at a lower ionic strength of 0.10 M ($pK_{a3} = 5.66$ and $pK_{a4} = 7.63$).[11] Combined, the ^{19}F NMR data obtained in the presence and absence of vanadate confirm that the V(V)−CF_2PP complex is exchanging rapidly.

Computational Evaluation of the Cyclic and Linear Products of the Reaction of Vanadate and Phosphate with PP_i and CF_2PP. One possible reaction pathway between

(53) Gerig, J. T. *Prog. Nucl. Magn. Reson. Spectrosc.* **1994**, *26*, 293−370.

Scheme 1.

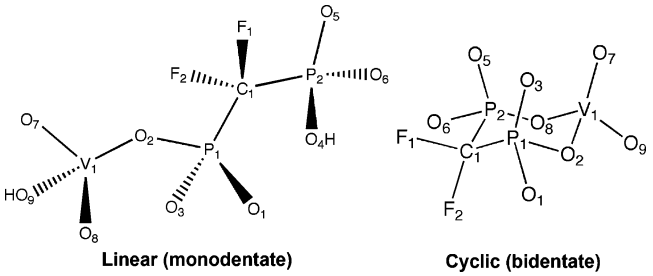

vanadate and $H[CF_2PP]^{3-}$ forming a 1:1 linear or cyclic complex (Scheme 1) is shown in eq 11.

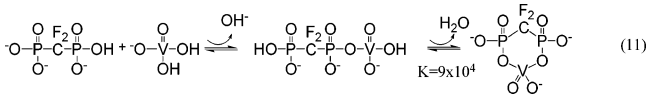

(11)

The reactants are protonated at one of the vanadate and phosphate oxygen atoms to model one of the most prevalent protonated form of CF_2PP and vanadate at pH 7. The calculated standard reaction free energy difference of −6.8 kcal/mol (55M H_2O, 298K, pH 7, see also Figure 4S) and the corresponding equilibrium constant of 9×10^4 mol/L strongly favor the cyclic product. The corresponding reaction of the trianionic PP_i (eq 12),

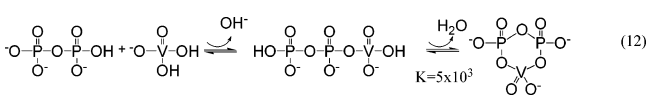

(12)

also shows a large preference for the bidentate complex, but the equilibrium constant, $K = 5000$ mol/L, is smaller than for CF_2PP analogue. To complete the comparison, we investigated the reaction of PP_i and CF_2PP with phosphate (eq 13).

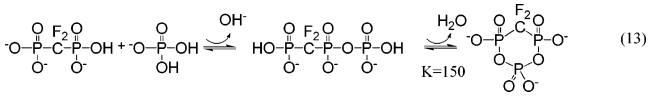

(13)

The equilibrium constant for the cyclization of CF_2-substituted triphosphate ($K = 150$ mol/L) was found to be similar to that for the parent triphosphate ($K = 90$ mol/L, eq 14),

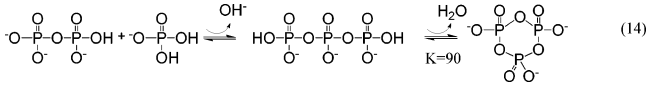

(14)

but significantly smaller than for the reactions with vanadate (eq 11 and 12). The cyclization of triphosphate, although predicted as favorable, may not be experimentally observable because of the competing spontaneous hydrolysis of triphosphate to PP_i. The hydrolysis side-reaction could be eliminated by studying equilibria for triphosphate with both bridging oxygen atoms substituted by CF_2. In nonaqueous solvents, a cyclic isomer of triphosphate has been detected as a product of reaction of *N*-cyclohexylphosphoramidate with pyridine.[54]

Since cyclization requires structural adjustments, these calculations provided some information on how these systems adjust to the steric limitations imposed by cation chelation. Importantly, the bridging P−O bond length in the linear calculated structure and in the crystal structure do not change as noted above when comparing the X-ray structure of the $H[CF_2PP]^{3-}$ anion to that of PP_i and chelated anions. In the cyclic $[VO_2CF_2PP]^{3-}$ complex (eq 11), the P−CF_2−P bite angle was found to change about 3°, but the major change in anion structure was the length of the P−O bond coordinated to the V. This geometric adjustment was also noted when comparing the geometry of the $H[CF_2PP]^{3-}$ anion structure with that of the Mg and V complexes reported previously. These studies therefore point to the possibility that the P−O bond length may be a key parameter in determining which metal ion chelators best assist in enzyme catalysis. Furthermore, they document that, as the metal ion radius increases, the stability of the cyclic adduct increase compared to a linear structure. These finding have consequences for binding of PP−metal chelates and also dictate when the application of vanadium as a transition state analogue in enzyme-catalyzed processes is possible.

Conclusion

A modified synthetic procedure for obtaining gram-scale amounts of pure difluoromethylene bisphosphonic acid was developed resulting in characterization of this fundamental structural unit analogous to PP_i. The X-ray structure of the tris-toludinium salt shows that the major structural differences are in the P−O bond length in the free CF_2 substituted anion and in complexes to metal ions. Although metal ion chelation has the potential to change this bite angle, comparison with X-ray data and theoretical evaluations suggest that the adjustments in the modified "PP_i" unit involve only minor bite angle changes.

The linear vanadate−PPi complexes are potential transition-state analogues in enzymes catalyzing nucleotide transfer or cyclization, for example, DNA polymerases or ATP cyclases.[55] The calculated relative stability of cyclic and linear forms of triphosphate and its isoelectronic vanadate−PP_i complex indicate that the vanadate−PP_i complex is much more favorable to bind to an enzyme in its cyclic form rather than analogous linear form. The replacement of the bridging oxygen of PP_i by the CF_2 group stabilizes the cyclic form rather than the linear form and thus is not a viable route for the design of vanadate-based transition state analogues of these systems.

2′-Deoxyribonucleoside triphosphate (dNTP) analogues containing the CF_2PP unit have been recently applied to study the mechanism of DNA replication. The observed differences in dNTP binding to human polymerase β with dNTP analogues[56] could be attributed to different abilities of leaving group chelation of metal ions, which are present in the enzyme active site. Our results document differences in structure and differences in chelation affinities of PP_i and CF_2PP. These combined measures may turn out to be useful when steric factors compromise the applications of dNTP analogues. The work described here suggests that simple chelation studies may assist mechanistic enzymology by providing metal chelation constants that combine the electronic and steric factors needed for dNTP−metal ion substrate recognition for many DNA processing enzymes. Further studies of other analogues will allow testing of such hypothesis.

Acknowledgment. We thank NIH for joint support to NICAS/NIH Grant No. 1U19CA105010. Additional support to J.F. was provided by the Research Corporation Research Innovation grant. We thank Samuel H. Wilson, Lars Pedersen, William Beard, Charles McKenna, and Arieh Warshel for stimulating discussions, and Dr. Bharat Baruah for technical assistance.

Supporting Information Available: Additional figures and tables. This material is available free of charge via the Internet at http://pubs.acs.org.

IC062484R

(54) Hamer, N. K. *J. Chem. Soc*. **1965**, 46−52

(55) Borden, J.; Crans, D. C.; Florián, J. *J. Phys. Chem*. **2006**, *110*, 14988−14999

(56) Sucato, C. A.; Upton, T. G.; Boris, A.; Kashemirov, V.; Martínek,; Xiang, Y.; Beard,. W. A.; Batra, V. K.; Pedersen, L. C.; Wilson, S. H.; McKenna, C. E.; Florián, J.; Warshel, A.; Goodman, M. F. *Biochemistry* **2007**, *46*, 461−471.